LCTp2-8L
Late-News Paper

Millimeter-Wave Reflective Liquid Crystal Phase Shifter Employing Two Strip Electrodes of Different Widths

Taichi Murai, Michinori Honma, Ryota Ito, and Toshiaki Nose

mhonma@akita-pu.ac.jp
Akita Prefectural University, 84-4 Tsuchiya-Aza-Ebinokuchi, Yurihonjo, Akita 015-0055, Japan
Keywords: liquid crystal, metasurface, millimeter-wave

ABSTRACT

In this study, we propose a liquid crystal (LC) millimeter-wave (MMW) metasurface with orthogonal wire-grid (OWG) electrodes having two different strip widths electrodes as a reflective LC MMW phase shifter that exhibits large phase variations. As a result, experimental verification confirmed that the reflection phase varies by up to 423°.

1 Introduction

In recent years, it has become possible to connect to the Internet through wireless communication systems in many aspects of daily life. Mechatronic devices such as robots, drones, and autonomous vehicles must control their position and motion using wireless communication systems. In such applications, ultra-high-speed, high-capacity, and low-latency wireless communication is desired. To realize high-performance wireless communication, it is necessary to use radio waves in frequency bands higher than MMW.

MMW has stronger directivity and greater atmospheric absorption compared to microwaves conventionally used in wireless communication systems, making the securing of line of sight (LoS) to avoid obstacles a critical issue. Moreover, since MMW needs to be efficiently directed to target locations and terminals, LC metasurfaces have attracted attention as RIS capable of controlling MMW propagation direction [1-5]. LC metasurfaces possess excellent characteristics including low driving voltage, low power consumption, lightweight, and compact structure, and can electrically control the phase and amplitude of MMWs. LCs exhibit large dielectric anisotropy in the MMW band, and when voltage is applied, the LC molecules reorient, resulting in significant changes in the dielectric constant [6].

LC-RIS can electrically control the reflection phase of MMWs by utilizing these properties of LC. To achieve a large beam-steering angle of an LC-RIS, a phase shift of at least 360° is required. For example, devices that achieve phase shifts exceeding 360° by arranging two different-sized metal patches functioning as resonators have been reported [5].

Previously, we proposed an OWG cell that functions as an LC-RIS [7]. The OWG cell has the feature that the influence of bias line installation on MMW reflection characteristics does not need to be considered since the strip array functions as both bias lines and electrodes. However, conventional OWG cells cannot achieve large phase shifts of approximately 360°. Therefore, to increase the phase shift, we adopted two resonator structures for the unit cell of the OWG cell, specifically using strip electrodes with different widths. In this study, we investigated the amplitude and phase characteristics of reflected waves in OWG cells with the proposed electrode structure.

2 Experimental Results and Discussion

Figure 1 shows the structure of the proposed OWG cell. For the top electrode, strip electrodes with different

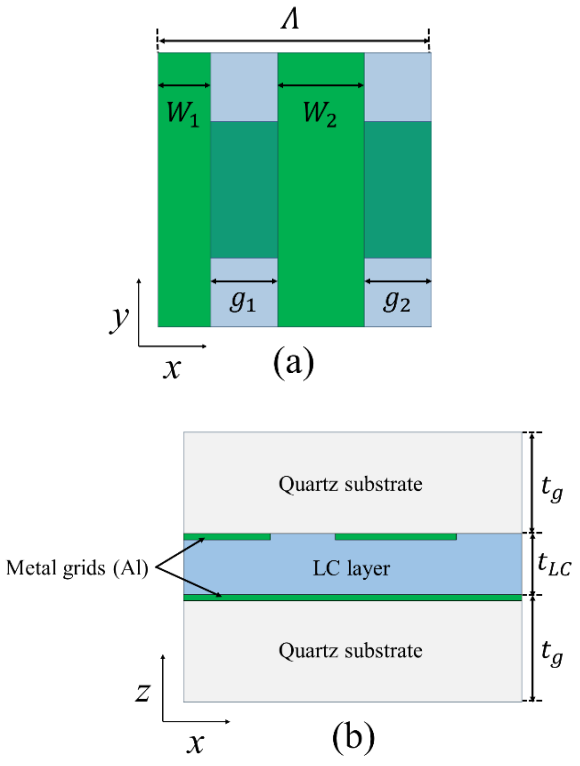

Fig. 1. (a) Top view and (b) side view of the unit cell of the proposed structure. W_1 and W_2 indicate the electrode widths; Λ, the array period; g_1 and g_2, the gaps; t_G, the substrate thickness; t_{LC}, the LC layer thickness.

widths were arranged in an array configuration. Meanwhile, for the bottom electrode, strip electrodes with a single width were positioned orthogonally. However, in this study, a single wide electrode was used instead of the strip electrode array for proof-of-principle experiments. The cell parameters are as follows: Λ = 4000 μm, W_1 = 1400 μm, W_2 = 1200 μm, g_1 = 700 μm, g_2 = 700 μm, t_{LC} = 100 μm, and t_G = 500 μm. The strip electrodes were fabricated using laser engraving technology on pre-deposited Al thin films (approximately 200 nm) formed by vacuum evaporation. Additionally, rubbed polyimide films were employed to achieve uniform LC alignment. The LC material used was ZOC-A018XX (JNC).

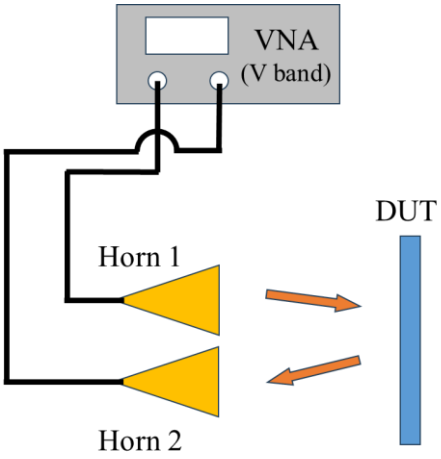

Fig. 2. Schematic of the measurement system for reflection characteristics of OWG cell using a VNA.

As shown in Figure 2, the reflection characteristics were measured using the conventional free-space method with a vector network analyzer (VNA) operating in the V band. The polarization direction of the incident wave was perpendicular to the grid on the side of the incident. The measurements were conducted over a frequency range of 40 to 65 GHz. A square wave voltage at 1 kHz was applied to the measured OWG cell.

Figure 3 shows the frequency-dependent waveforms of the reflection coefficient with and without applied voltage. The waveforms measured under both conditions exhibit dips due to resonance. The resonant frequency shifted to lower frequencies due to the increase in the dielectric constant of the liquid crystal layer upon voltage application. In conventional OWG cells, when voltage is applied, the resonant frequency shifts to lower frequencies while maintaining the same waveform shape. However, as shown in Figure 3, the proposed OWG cell exhibited a change in its waveform. When no voltage was applied, the waveform dip became sharp, essentially producing only a single resonant frequency (55.3 GHz). When voltage was applied, the bottom of the resonant frequency dip became flat. This suggests a state where two resonant waveforms are superimposed. Although the exact resonant frequency is not clearly defined in this case, Fig. 3 indicates that the resonant frequency lies within the range of 49 to 53 GHz.

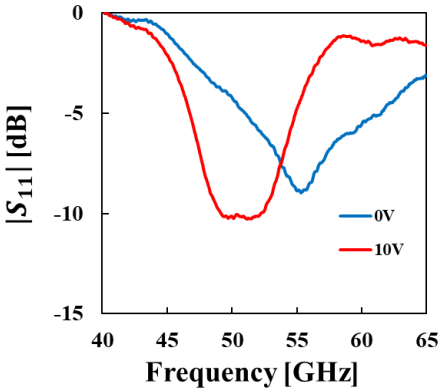

Fig. 3. Magnitude of the reflection cofficient of the OWG cell, where Λ = 4000 μm, W_1 = 1400 μm, W_2 = 1200 μm, g_1 = 700 μm, g_2 = 700 μm.

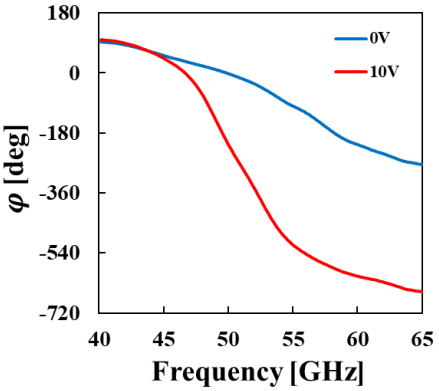

Fig. 4. Reflection phase characteristics of the OWG cell, where Λ = 4000 μm, W_1 = 1400 μm, W_2 = 1200 μm, g_1 = 700 μm, g_2 = 700 μm.

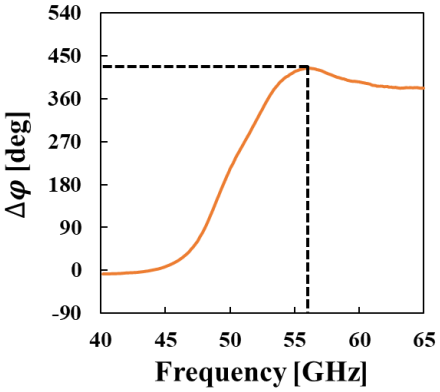

Fig. 5. Relationship between the frequency and the reflection phase change $\Delta\varphi$, which was calculated from reflection phase characteristics of Fig. 4.

Figure 4 shows the reflection phase with and without applied voltage. When no voltage was applied, the phase decreased by 366° as the frequency varied from 40 to 65 GHz. In contrast, when voltage was applied, the phase decreased by 754°. Upon voltage application, the phase reduction with frequency variation became significantly larger compared to the condition without voltage. Without voltage application, the phase reduction was small due to essentially a single resonance. Conversely, after voltage application, the phase reduction was large because two different resonant frequencies were occurring simultaneously.

Figure 5 shows the phase shift characteristics when voltage is applied. $\Delta\varphi$ was defined by the following equation:

$$\Delta\varphi = \varphi_{10} - \varphi_{0}. \quad (1)$$

φ_0 and φ_{10} denote the reflection phases at applied voltages of 0 V and 10 V, respectively. From the figure, a maximum phase change of 423° was obtained at 56.1 GHz.

3 Conclusions

We proposed a MMW reflective LC phase shifter using a unit cell composed of two strip electrodes with different widths. It was demonstrated that large phase shifts can be obtained by simultaneously generating resonances at two different resonant frequencies that are slightly offset from each other.

4 Acknowledgments

The authors are grateful to JNC Corporation, Japan, for providing the nematic LC material ZOC-A018XX for the MMW applications. This work was partially supported by the Ministry of Internal Affairs and Communications (MIC), Japan, through the FORWARD Program for Beyond 5G Promotion (JPMI250210005).

References

[1] H. Matsuno, T. Ohto, T. Hayashi, Y. Amano, M. Okita, and D. Suzuki, IEEE Access, vol. 11, pp. 95757-95767 (2023).

[2] Y. Youn, D. An, D. Kim, M. Hwang, H. Choi, and B. Kang, IEEE Antennas and Wireless Propagation, vol. 71, pp. 9415-9423 (2023).

[3] T. N. Lang, Y. Inoue, and H. Moritake, IEICE Communications Express, vol. 13, pp. 235-239 (2024).

[4] M. Sode, M. Ponschab, L. N. Ribeiro, S. Haesloop, E. Tohidi, and M. Peter, IEICE Access, vol. 12, pp. 163155-163171 (2024).

[5] Y. Cui, H. Sato, K. Xu, H. Fujikake, and Q. Chen, IEEE Antennas and Wireless Propagation Letters, Vol. 23, pp. 3529-3533 (2024).

[6] T. Nose, S. Sato, M. Honma, T. Nozokido, and K. Mizuno, Applied Optics, vol. 44, pp. 1150-1155 (2005).

[7] M. Honma, T. Okamoto, R. Ito, and T. Nose, Proceedings of the international Display Workshops, vol. 31, pp. 56-58 (2024).